Russian winter and spring wheat productivity, heat stress and drought conditions at flowering, and the role of atmospheric blocking

Paraskevi Giannakaki[1], Pierluigi Calanca[1]

[1]Agroscope Research Division, Agroecology and Environment,
Reckenholzstrasse 191, 8046 Zurich, Switzerland

Correspondence to: Paraskevi Giannakaki (paraskevi.giannakaki@gmail.com)

Abstract. Russia has become the foremost wheat exporting country worldwide. Episodic production breakdowns caused by extreme weather during sensitive stages of crop development are hence of concern not only for the domestic but also for the global wheat market. In this study, we examine heat stress occurrence and availability of rainwater during the flowering period, and investigate their impacts on the winter and spring wheat yields of three major production areas of Russia. We also consider the role of atmospheric blocking as a precursor of extreme weather and assess the correlation between blocking duration and yield. Owing to the later occurrence of flowering in spring wheat and the warmer climate of Southern European Russia, we find the probability of heat stress to be higher in spring than in winter wheat, and higher in the south than in the north of the study area. For spring wheat, the negative association between yield and heat stress is stronger than the positive association between yield and total precipitation. The reverse is true for winter wheat. In all regions and for both wheat types, heat stress occurrence and total precipitation amounts correlate significantly with the area-weighted average of blocked days. We also find correlation between blocking duration and yield, but results are significant only for spring wheat.

KEY WORDS: wheat, atmospheric blocking, heat stress, drought, Russia

1 Introduction

The Russian Federation considerably increased its wheat exports during the recent past, becoming in 2016 the leading wheat exporter worldwide (United States Department of Agriculture 2016). Episodic production collapses in Russia can therefore have considerable repercussions on the global wheat market (Zampieri et al. 2017). This occurred in 2010, when a large fraction of the wheat cultivation area of Russia, experienced extraordinary high temperatures throughout the summer (Grumm 2011; Barriopedro et al. 2011; Dole et al. 2011; Wright et al. 2014; Katsafados et al. 2014; Russo et al. 2015). Consequently, harvested grains dropped off by about 40% from previous years' levels, whereupon the Russian government issued a wheat export ban that lasted until mid of 2011 and led to an upsurge in global prices of up to 50 % (Food and Agriculture Organization of the United Nations 2010; Welton 2011).

Exposure to high temperatures is recurrent in the main wheat production area in the south-west of Russia. Since most of the cultivation is rainfed, lack of precipitation can also limit production (Alcamo et al. 2007; Daryanto et al. 2016). Not all development stages of wheat are very sensitive to water shortage (Brouwer et al. 1989), but water shortage occurring in the time from booting to early grain formation can depress yields (Schneider et al. 1969; Mogensen et al. 1985). Even more harmful than drought alone is the co-occurrence of heat stress and drought (Nicolas et al. 1984), a situation that was responsible for the severe production losses suffered in 2010 (Lupo et al. 2014).

Heat stress, often in association with water shortage, is particularly harmful to wheat if it occurs at flowering (Brouwer et al. 1989; Wheeler et al. 2000; Wollenweber et al. 2003). Production losses caused by temperatures in excess of critical thresholds during this phase of development can indeed be considerable (Fontana et al. 2015). In global investigations of the exposure of crops to damaging temperatures during the reproductive period (Gourdji et al. 2013; Teixeira

et al. 2013) some areas within the Russian Federation appear as hot spots. Yet, without addressing the problem at the regional scale, it is not possible to provide detailed information on the recurrence of heat stress and drought conditions. Another limitation of global studies is that they consider wheat as a crop in a generic way without making a distinction between winter and spring varieties, though this is vital in this context, as the two varieties flower asynchronously.

In this paper, we assess the occurrence of high temperature and low precipitation amounts in the reproductive period based on local weather data, and examine their association to winter and spring wheat yield variations at the regional scale based on official yield statistics.

Atmospheric blocking events are among the large-scale flow patterns that favour the occurrence of extreme heat and drought (Tyrlis & Hoskins 2008; Petoukhov et al. 2013). The presence of long-lasting anticyclones during the growing season of wheat is not unusual in Russia (Park & Ahn 2014; Antokhina et al. 2016). A second objective is therefore to provide a statistical analysis of the influence of atmospheric blocking on the occurrence of heat stress and drought conditions in the reproductive period of wheat and to evaluate in a direct way the correlation between the duration of atmospheric blocking and wheat yield, again considering winter and spring varieties separately.

2 Data and data processing

2.1 Daily weather data

The analysis relies on 118 land-based weather stations distributed across the wheat production area of Russia (Figure 1). The database includes daily minimum (T_{min}), and maximum temperature (T_{max}), and daily precipitation amounts (Pr) in liquid water equivalent. The data were obtained from the Carbon Dioxide Information Analysis Centre (CDIAC) for the period

1980-2009 (Bulygina & Razuvaev 2012) and the Federal Service of Hydrometeorology and Environmental Monitoring (2008) for the period 2010-2014.

A data quality control was performed using the RClimDex tool (Zhang et al. 2004) to eliminate unreasonable values (i.e. $Pr < 0$ and $T_{max} < T_{min}$). The test also checked for temperature values outside a range given by the climatological daily mean ± 3 times the corresponding climatological daily standard deviation, individually for each of T_{min} and T_{max}.

2.2 Blocking Index

To quantify the occurrence of blocking situations, we adopted the two-dimensional Blocking Index (*BI*) of Rohrer et al. (2018), which is available at $2° \times 2°$ spatial resolution and 6-hourly temporal resolution. The *BI* was computed from 6-hourly ERA-interim re-analyses of the 500 hPa geopotential height (*z500*) for 1979-2015 (Dee et al. 2011), based on the blocking detection algorithm of Lejenäs and Økland (1983), Tibaldi and Molteni (1990) and Tibaldi et al. (1994). For a given latitude $\boldsymbol{\varphi}$ between $36° - 76°$ North or South, the algorithm checks whether:

1) The *z500* gradient towards the pole $= \frac{z500_{\varphi+14} - z500_{\varphi}}{14} < -10 \frac{gpm}{{}^{\circ}lat}$ and
2) The *z500* gradient towards the equator $= \frac{z500_{\varphi} - z500_{\varphi-14}}{14} > 0 \ \frac{gpm}{{}^{\circ}lat}$

A blocking condition is detected when areas characterized by a reversal of the meridional *z500* gradient have a spatial overlap of more than 70% during at least five consecutive days (Schwierz et al. 2004; Scherrer et al. 2006). The binary BI is the result of assigning a value of one when all conditions are satisfied, and of zero otherwise.

2.3 Yield

Yield statistics for winter (*WW*) and spring wheat (*SW*) for the period 1995-2014, as compiled at the provincial level by the Federal State Statistics Service of Russia, were obtained from

Schierhorn et al. (2014) along with statistics of the corresponding sowing area for the period 1995-2009. The data were complemented with information available from the Statistical Handbooks of the Russian Statistics Service (Russian Federal State Statistics 2014; Russian Federal State Statistics 2016).

2.4 Wheat phenology

As in Trnka et al. (2014), wheat phenological development was estimated with the help of the empirical model of Olesen et al. (2012). The model calculates the duration of phenological phases as:

$$S = \sum \max(T_i - T_b, 0) \cdot \alpha_i \quad (1)$$

where S is the temperature sum required to complete the given phase, T_i is the daily mean temperature, T_b is the base temperature and α_i is a daily photoperiodic response. The model assumes that the latter is relevant only in the period from emergence until flowering and gives α_i as:

$$\alpha_i = \min\left\{\max\left[\frac{(\lambda_i - 7)}{13}, 0\right], 1\right\} \quad (2)$$

where λ_i is the daylength on day of the year i, obtained from latitude using standard astronomical formulas (e.g. Allen et al. (1998)).

For winter wheat, the summation in (1) starts on first of January, whereas for spring wheat it starts at sowing, i.e. on the first date of the year when the average temperature over a 10-day period exceeds a threshold T_s.

The model sets T_b equal to 5°C in all cases, but the temperature sum requirements, S, are specified as a function of the long-term mean annual temperature, to reflect the fact that current

wheat varieties are already chosen to match local climatic settings (Olesen et al. 2012). For similar reasons, the model also expresses the temperature threshold T_s as function of latitude (see Olesen et al. 2012 for details).

2.5 Probability of heat stress and total precipitation at flowering

The occurrence of adverse weather conditions in the reproductive period was gauged by computing the probability of heat stress (p_{HS}) and total precipitation amounts (tPr) for the 31 days centred on the date of flowering (DOY_{flo}).

In a first step, a binary indicator of heat stress occurrence (I_{HS}) was computed for each station and day as:

$$I_{HD} = \begin{cases} 1 & if\ T_d > T_{crit} \\ 0 & otherwise \end{cases} \quad (3)$$

where $T_{crit} = 27°C$ is the critical temperature (Teixeira et al. 2013), and T_d is the daytime temperature. The latter was estimated from T_{min} and T_{max} by integrating in time the equation for approximating hourly temperatures derived by Felber et al. (2018), viz.:

$$T_d = \frac{1}{h_S - h_R - c} \int_{h_R - c}^{h_S} T_h \, dh =$$

$$= T_{min} + (T_{max} - T_{min}) \frac{h_S - h_R + 2a - 2c}{\pi(h_S - h_R - c)} \left\{1 - cos\left[\frac{\pi(h_S - h_R - c)}{h_S - h_R + 2a - 2c}\right]\right\} \quad (4)$$

where T_h is the temperature at hour h, h_S and h_R are sunset and sunrise hours calculated for each station based on the station's latitude and the day of the year, $a = 2.5$ and $c = 0.5$ (Parton & Logan 1981; Felber et al. 2018)

With (1) the probability of heat stress was reckoned as:

$$p_{HS} = \frac{1}{31}\sum_{DOY_{flo}-15}^{DOY_{flo}+15} I_{HD} \quad (5)$$

where DOY_{flo} is the estimated date of flowering.

In similar fashion, total precipitation at flowering was evaluated as:

$$tPr = \sum_{DOY_{flo}-15}^{DOY_{flo}+15} Pr \quad (6)$$

2.6 Spatial aggregation of the weather and yield data

For the statistical analysis of a possible association between heat stress and drought conditions and wheat yield variability, we spatially aggregated weather and yield data. We identified groups of stations with similar characteristics as of the occurrence of high temperatures by means of cluster analysis. Clustering was implemented following Bador et al. (2015) based on a Partitioning Around Medoids (*PAM*) approach (Gentle et al. 1991; Bernard et al. 2013) and using the 90th percentile of T_{max} as a similarity target.

Compared to the more common *K-means* clustering algorithm (Hartigan & Wong 1979; Hartigan et al. 1981), *PAM* has the advantage of preserving the maxima in each cluster, being therefore consistent with extreme value theory (Coles 2001). As a measure of distance between clusters, the F-Madogram was used (Cooley et al. 2006). The analysis was implemented in R by means of the package SpatialExtremes (Ribatet et al. 2011), with optimal number of clusters being determined according to an average silhouette coefficient that contrasts cluster tightness with cluster dissociation.

Results of the analysis indicated two clusters as optimum solution, a Northern Cluster (*NC*) containing 77 stations essentially located north of $50° N$, and a Southern Cluster (*SC*) with 41 stations located in Southern European Russia and Southern Siberia. By examining the probability of heat stress occurrence in relation to atmospheric blockings, we found it reasonable to further split the *NC* along the Ural Mountains (approximately $60° E$) into a Western (*NCW*) and Eastern Cluster (*NCE,* Figure 1).

Although the clustering process primarily targets extreme temperatures, the results are consistent with the Geiger-Köppen climate classification, which displays *Dfa* climates (humid snow climates with hot summer) in the south and *Dfb* climates (humid snow climates with warm summers) in the north (Kottek et al. 2006; Peel et al. 2007). They are also consistent with the the agroclimatic zonation of Bulgakov et al. (2016),which shows dominance of winter wheat cultivation in the *SC*, but of spring wheat cultivation in the *NC*.

Finally, results of the cluster analysis also more or less follow the political division of the Russian territory, with the *NCW* corresponding to large extend to the Central and Volga Federal Districts, the *NCE* to the Ural and the southern part of the Siberian Federal Districts, and the *SC* to the Southern Federal District. Because of this, we used the political borders as limits for the spatial aggregation of the yield data, employing the sown area as a weighting factor for the averaging process.

2.7 Temporal and spatial aggregation of the Blocking Index

To obtain a suitable indicator of blocking activity, we aggregated the 2-dimensional fields of Rohrer *et al.* (2018) over two spatial domains,: the first one spanning the area delimited by $30 - 60° E$ and $45 - 60° N$, the second the area delimited by $60 - 90° E$ and $45 - 60° N$.

The size and location of the areas are consistent with those assumed by Schaller et al. (2018) for examining the influence of blocking on Western Russian heatwaves. Here, we considered the first domain as being representative of blocking anticyclones affecting the *NCW* and *SC*, the second one as connotative of blocking systems affecting the *NCE*.

Analogously to Schaller et al. (2018), we calculated for both domains the area-weighted average of blocked days (*ABD*), which was taken as blocking indicator for correlation analysis. *ABD* is the result of spatially averaging the number of positive counts of the *BI* during the 31 days around flowering ($DOY_{flo} - 15$ to $DOY_{flo} + 15$).

3 Results

3.1 Weather conditions at flowering and wheat yields

We calculated flowering to occur from end of May to mid-June in winter wheat and from mid-June to mid-July in spring wheat (Figure 2). This is in line with the crop calendars published by the US Department of agriculture (United States Department of Agriculture 2006; 2017) and the data extracted from the report prepared by Savin et al. (2007). In the *SC* flowering occurred earlier than in the *NC*, especially in the case of spring wheat. Within the *NC* spring wheat flowering in the western part happened a few days earlier than in the eastern part. For winter wheat, the differences in DOY_{flo} between the *NCW* and the *NCE* were minor.

In general, the *SC* experienced higher daytime temperatures than either the *NCW* or the *NCE* (supplementary Figure S1), the excess being of about 2℃ for both wheat types.

225 Total precipitation amounts during the flowering period of winter wheat were of about $56\ mm$
226 ($sd = 20.8\ mm$) in the *NCW* and of $50\ mm$ ($sd = 18\ mm$) in the *NCE* and the *SC*.
227 Corresponding area averaged amounts for the flowering period of spring wheat were higher:
228 namely $71\ mm$ ($sd = 26.6\ mm$), $62\ mm$ ($sd = 15.9\ mm$) and $56\ mm$ ($sd = 18.9\ mm$) in
229 the *NCW, NCE* and *SC,* respectively.

230

231 Concerning yield, spatial aggregation of the provincial statistics indicated area-mean
232 productivity levels of $22.0, 18.8$ and $26.1\ dt\ ha^{-1}$ for winter wheat, and of $17.8, 13.8$ and
233 $9.1\ dt\ ha^{-1}$ for spring wheat, in the *NCW*, *NCE* and *SC*, respectively (Table 1). For both wheat
234 types and all clusters, the within-cluster coefficient of variation was approximately 25%, in
235 line with the findings of Zampieri et al. (2017).

236

237 At the annual level, largest yield deficits occurred in 1998, varying, depending on region,
238 between -30 and -60% in the case of winter wheat, and between -40 and -80% in the case of
239 spring wheat (Table 1). Yields were again low in 2010, falling short of the average by more
240 than 30% in the case of winter wheat, and by more than 40% in the case of spring wheat in the
241 west of the study area (*NCW* and *SC*). The results suggest that the 2010 heat wave had only
242 minor effects on wheat production to the east of the Ural Mountains.

243

244 **Table 1: Yield statistics valid for 1995-2014, and yield anomalies in 1998 and 2010.**

yield 1995-2014	winter wheat			spring wheat		
	NCW	*NCE*	*SC*	*NCW*	*NCE*	*SC*
mean (dt ha^{-1})	22.0	18.8	26.1	17.8	13.8	9.1
st. dev. (dt ha^{-1})	6.3	5.3	7.1	4.8	3.7	2.4
Coefficient of variation	28.7%	28.1%	27.1%	26.8%	26.8%	26.1%
anomaly 1998 (dt ha^{-1})	-7.68	-10.68	-7.44	-10.3	-5.05	-7.07
anomaly 2010 (dt ha^{-1})						

	-7.37	-5.06	-5.56	-7.92	-0.95	-4.15

245

246 **3.2 Probability of heat stress, precipitation and their association to yield variability**

247 Our analysis indicates that sites frequently exposed to high temperatures were mostly located
248 in the *SC* (supplementary Figure S2). The probability of heat stress was higher in spring than
249 winter wheat owing to differences in the time of development (Figure 2).

250

251 Regional differences also appear in relation to total precipitation amounts for the 31-day
252 window around the flowering date (supplementary Figure S3). According to our evaluation,
253 stations with the highest probability of heat stress also displayed the lowest total precipitation
254 amounts. *NC* stations received more precipitation than *SC* stations and precipitation amounts
255 were slightly higher for spring than for winter wheat.

256

257 Results of the correlation analysis of yields against probability of heat stress and total
258 precipitation amounts are presented in Table 2 and in Figures 3 and 4. In view of the relatively
259 small sample size (time series of yield span only 20 years) and because data cannot be assumed
260 to stem from a bivariate normal distribution, we quantified the level of association by means of
261 Spearman rank correlation, a more robust metrics that the ordinary Pearson correlation
262 coefficient (Press et al. 2007).

263

264 Heat stress probability in the reproductive period did not explain winter wheat yield variations
265 in the *NCW* and the *SC*. We found however, a significant negative correlation between yield
266 and probability of heat stress for winter wheat in the *NCE* and for spring wheat in all clusters.
267 Regarding the association of wheat yield variations with total precipitation, we obtained
268 significant positive correlations for both winter and spring wheat in the *NCE* and for winter
269 wheat in the *SC*. Results were not significant for the *NCW*.

For winter wheat, there was a significant correlation between probability of heat stress occurrence and total precipitation amounts in the *NCW* and *NCE* and for spring wheat, in the *NCW* and *SC* (supplementary Table S1).

Table 2: Spearman rank correlation between probability of heat stress, respectively total precipitation and wheat yields. Bold face: statistically significant results. Significance levels: (*) 10%, (**) 5%, (***) 1%. Results for the one-side test of a negative (p_{HS}), respectively positive (tPr) association against the null hypothesis of no association.

	Winter Wheat				**Spring Wheat**		
	NCW	*NCE*	*SC*		*NCW*	*NCE*	*SC*
p_{HS}	-0.02	**-0.72 (***)**	-0.28		**-0.47 (**)**	**-0.56 (**)**	**-0.47 (**)**
tPr	0.31	**0.68 (***)**	**0.53 (**)**		0.24	**0.46 (**)**	0.37

The lack of correlation between probability of heat stress at flowering and winter wheat yield variations in the *NCW* can be understood bearing in mind the early date of flowering and the relatively low temperatures occurring in this cluster at this time of the year. The lack of correlation between winter wheat yield variations and occurrence of heat stress in the *SC* (Figure 3) is less obvious and further discussed in Section 4. A priori, however, numerical problems arising from uncertainties in the specification of the critical temperature thresholds (which depends on wheat variety) or in the estimation of the date of flowering cannot be excluded.

To ascertain a possible impact of uncertainties in the date of flowering, we carried out a simple sensitivity analysis, that consisted in subtracting 5 days and adding 5 and 10 days to the estimate obtained with the Olesen et al. (2012) model and reassessing the statistics. We found that shifting the date of flowering had minor effects on the correlation coefficients calculated for

spring wheat (all cluster) as well as for winter wheat in the *NCW* and *NCE (supplementary Table S2)*. However, it affected the correlation coefficient and its statistical significance in the case of winter wheat in the *SC*. In this case, the assumption of later dates of flowering resulted in a higher correlation coefficient.

3.3 Links to blocking

The time series plotted in Figure 5 and supplementary Figures S4 and S5 demonstrate the distinct exposure to blocking conditions in the different clusters. Long-term mean *ABD* values ranged from about 1 day in the *NCE* to about 3 days in the other two clusters. In the *NCW* and *SC*, the average number of blocked days was slightly higher during the flowering season of *WW* than during that of *SW*. The inter-annual variability of the average number of blocked days was large in all cases. In the *NCW* and the *SC*, the standard deviation of *ABD* was around 2 days for winter wheat, and around 1 day for spring wheat. For the *NCE,* the standard deviation was around 1 day for both wheat types. Overall, these results reflect the different dynamical and climatological characteristics of blocking situations occurring to the east and to the west of the Ural mountains (Matsueda 2011; Cheung et al. 2013; Dunn-Sigouin & Son 2013).

With respect to winter wheat in the *SC*, and to spring wheat in the *NCW* and the *SC*, the variability in blocking activity explained about 40% of the inter-annual variability in probability of heat stress at flowering (supplementary Figure S4 and Table 3). Blocking was also largely responsible for precipitation variations in the *NCW* (supplementary Figure S5 and Table 3). In this case, the share of explained variance was less important in the *NCE* (around 20% for both wheat types) and the *SC* (14% in *WW* and 24% in *SW*).

Table 3: Spearman rank correlation between average number of blocked days and (top to bottom) heat stress, total precipitation and weighted yield. Bold face: statistically significant results. Significance levels: (*) 10%, (**) 5%, (***) 1%.

	Winter wheat				Spring wheat		
	NCW	*NCE*	*SC*		*NCW*	*NCE*	*SC*
p_{HS}	**0.53 (***)**	**0.44 (***)**	**0.62 (***)**		**0.74 (***)**	**0.43 (***)**	**0.76 (***)**
tPr	**-0.73 (***)**	**-0.48 (***)**	**-0.38 (**)**		**-0.79 (***)**	**-0.42 (***)**	**-0.49 (***)**
Weighted yield	-0.33	-0.36	-0.37		**-0.54 (**)**	-0.36	**-0.57(***)**

For spring wheat, year-to-year variations in the average number of blocked days explained around 30% of the observed yield variations in the *NCW* and *SC* and 13% in the *NCE* (Figure 5 & Table 3). For winter wheat, the correlation coefficients were lower and overall statistically not significant.

An interesting feature emerging from Figure 5 is the fact that, except for spring wheat in both the *NCW* and the *SC*, the average number of blocked days estimated for 2010 was close or even below the long-term average. This contrasts with the situation in 1998, a year for which the average number of blocked days fell in the upper tail of the distribution for both wheat types and all clusters. One possible explanation for the unexpected result concerning 2010 was the geographic position of the atmospheric blocking systems during spring season (Dole et al. 2011). In fact, it was only during June, i.e. the flowering time of *SW* that persistent high-pressure centres settled close to the western border of the study area.

4 Discussion and Conclusion

The sensitivity of wheat to extreme high temperature and water shortage around flowering makes wheat cultivation particularly vulnerable to heat waves that occur at this stage of development (Wheeler et al. 2000; Gourdji et al. 2013). A first goal of our study was to quantify the correlation between the probability of heat stress occurrence and total precipitation in the

reproductive period with yield, based on regional yield statistics. A second goal was to investigate the role of atmospheric blocking as a determinant of extreme weather conditions during flowering and eventually also with yield.

Because we were not able to obtain actual phenological data, we employed the phenology model of Olesen et al. (2012) to estimate the dates of flowering. We showed that the model output is in line with agronomic information available from independent sources, for example the crop calendar published for the Russian Federation by the International Production Assessment Division of the Foreign Agricultural Service of the USDA (United States Department of Agriculture 2017). Lack of phenological data from Russia precluded a direct model validation, implying that, our estimates are uncertain. In view of this, we recommend the collection of historical and current phenological data from all over Russian arable areas as a primary task for the future.

Our work confirms the crucial role of heat stress and water shortage for Russian wheat production, supporting the conclusion of Zampieri et al. (2017) that heat stress can explain a large fraction of the variability in winter wheat yields observed for Russia at the national scale. However, the correlation was significant only for the *NCE*, which suggests that other determinants are need to be taken into account in the other regions.

For spring wheat, on the other hand, we found significant correlations between heat stress and yield for all regions. In spring wheat, flowering occurs later in the year, and temperatures are generally higher than during the flowering period of winter wheat. We therefore expect higher levels of heat stress and a higher incidence on yield in spring wheat than winter wheat.

Concerning the link between precipitation amounts at flowering and yield, significant high correlations were established in the *SC* and the *NCE* for both wheat types, reflecting the fact that aridity patterns are more persistent in time (and space) and therefore more coherent between winter and spring wheat (Fig. S3).

We ascertained that the probability of heat stress is particularly important in the Southern and Central Federal Districts. The former region is the most important cultivation area with respect to winter wheat; the second contributes significantly to spring wheat production. It is also important to bear in mind that heat stress and water shortage usually occur in sympathy, which magnifies the negative impacts of these two types of stress taken individually (Nicolas et al. 1984). Indeed, correlation coefficients between heat stress and water shortage were in many cases significant (Table S1). Years characterized by a high probability of heat stress and low precipitation in the present analysis (in particular 1981, 1998 and 2010) are also identified in the compilation of historical drought events and heat waves prepared for Eurasia by Schubert et al. (2014).

For Russia, previous studies proposed atmospheric blocking as a precursor of extreme weather (Grumm 2011; Schneidereit et al. 2012; Antokhina et al. 2016). The role of blocking as a driver of warm spell is in fact well established (Pfahl & Wernli 2012; Brunner et al. 2017; Schaller et al. 2018). Our analysis confirmed that for Russia's wheat production area, blocking activity had a systematic influence on the occurrence of adverse weather conditions at flowering, explaining between 20 to 60% of the inter-annual variability of heat stress and water availability at flowering in the time since 1980.

The results suggest regional differences between the impacts of European blocking systems on wheat production in the north-west and south of Russia, and the repercussions of Ural blocking

391 systems on wheat production in the northeast. We found in particular a significant negative
392 correlation of around -0.6 between the spring wheat variability and blocking activity for the
393 *NCW*, *SC* and -0.4 for the *NCE*.
394
395 The lack of correlation between blocking activity and probability of heat stress with respect to
396 winter wheat production in Southern Russia is in any case surprising. Apart from possible
397 problems in assessing the date of flowering (see above), the absence of a negative association
398 could also reflect the rapid expansion of the cultivated area that has taken place in the last two
399 decades and efforts undertaken to intensify winter wheat production in the areas offering the
400 highest production potentials (Schierhorn et al. 2014). It could also reflect the fact that also frost
401 and heavy rains are often the cause of damages. Frost and heavy rains have been recurrent in
402 the recent past in southern Russia, as documented e.g. in the Commodity Intelligence Report
403 on the Russian Federation by the International Production Assessment Division (IPAD) of the
404 Foreign Agricultural Service of the USDA (United States Department of Agriculture 2018). An
405 interesting future study would therefore be to examine the role of blocking during winter and
406 early spring season, connected with cold spells (Sillmann et al. 2011; Brunner et al. 2017),
407 taking into account key agronomic and production data.
408
409 A chief premise of our study was that wheat is particularly sensitive to heat stress during
410 flowering (Brouwer et al. 1989; Wheeler et al. 2000; Wollenweber et al. 2003). Implicitly we
411 assumed that limiting the attention to a short period (31 days around flowering) was adequate
412 for the purpose of uncovering statistically significant relations. It is possible however, that it
413 would have been more suitable to consider the entire growing season. To address this, we
414 repeated the analysis aggregating all relevant data over days of the year 121-212 for *WW* (May-
415 Jul); and days 152-243 for *SW* (Jun-Aug, http://www.amis-outlook.org/amis-
416 about/calendars/en/). Correlations were neither higher nor statistically more significant than we

found with periods used in the main analysis. However, we used the 31-days window around blooming to be consistent with previous assessments (Teixeira et al. 2013; Gourdji et al. 2013).

Russian wheat production could benefit from early warning systems that help limiting the negative impacts of extreme weather on crop development. A better physical understanding of the link between atmospheric blocking and extreme heat would certainly support such a system. This requires addressing teleconnection patterns as precursors of blocking situations, on the one hand, and heat-waves and droughts on the other hand (Renwick & Wallace 1996; Shabbar et al. 2001; Barriopedro et al. 2006; Rust et al. 2014; Folland et al. 2009; Casanueva et al. 2014; Scherrer et al. 2006).

During the summer season teleconnection patterns are weaker but they have been proven to have strong links with temperature and precipitation conditions in Eurasia (Rust et al. 2014; Folland et al. 2009; Irannezhad & Kløve 2015; Irannezhad et al. 2016). Other studies demonstrated that different phases of El Niño-Southern Oscillation (which is usually perceived more clearly during boreal winter) are statistically related to spring and summer temperature and precipitation anomalies in Russia (Mokhov & Timazhev 2017; Mokhov & Semenov 2016). Further work is hence required to clarify the interdependence of blocking activity, with large-scale circulation anomalies and with El Niño phases in the areas that support Russian wheat production.

For the present investigation, we opted for a binary blocking index that quantifies blocking occurrence without addressing the multifaceted nature of blocking dynamics including intensity, location, and life-cycle of individual blocking events. Additional work addressing these aspects could help explaining the causal relations leading to adverse conditions for wheat cultivation, eventually reducing the vulnerability of Russian agriculture to extreme weather events.

In principle, expanding production areas to the North (Fischer et al. 2002; Schierhorn, Faramarzi, et al. 2014; Liefert & Liefert 2015; Di Paola et al. 2018; Belyaeva & Bokusheva 2018) or changing wheat types and/or varieties could be a measure to avoid production shortfalls caused by critically high temperatures. Yet, in practice, the risk of incurring in production shortfalls caused by heat stress would remain substantial (Dronin & Kirilenko 2008).

Looking forward, an important question for Russian agriculture is the one of a possible future increase in blocking activity. Mokhov & Timazhev (2015) studied the likelihood of future occurrences of northern hemisphere blocking episodes from the perspective of different emission and climate scenarios and concluded that a tendency for an increase in the duration of blocking events is very likely.

Conclusions of retrospective studies are, however, less categorical in this respect. Barnes et al. (2014) found for example that no clear increase in blocking could be detected over 1980-2012 irrespective of the data and indices used. Rather they noticed that blocking exhibits large variations and that it is difficult to discriminate between the contribution from internal variability and external forcing. Candidates for the latter are e.g. a weakening summer circulation in the Northern Hemisphere mid-latitudes (Coumou et al. 2015) or changes in the Atlantic Multidecadal Ocean Variability (Häkkinen et al. 2011).

Consistent with this, Dunn-Sigouin & Son (2013) concluded that even under the constraints of the RCP 8.5 emission scenarios, expected changes in the number and duration of blocking events under future climatic conditions will likely be insignificant. Clearly, there is still considerable uncertainty in projections of blocking activity under future climate scenarios (Woollings et al. 2014), which stresses the need for additional investigations.

Acknowledgements

The authors are grateful to Dr. Florian Schierhorn for providing yearly wheat data and Dr. Marco Rohrer for providing blocking index data. We acknowledge the time and effort devoted by reviewers to improving the quality of this paper. We also acknowledge the free availability of data sets from the CDIAC and ROSHYDROMET (land-based weather station data) and the contributors of R software. We obtained financial support from the Swiss National Science Foundation with Grant No. IZRPZ0 164737.

References

Acevedo, E., Silva, P. & Silva, H., 2002. Wheat growth and physiology. *BREAD WHEAT Improvement and Production*, p.544. Available at: http://www.fao.org/docrep/006/Y4011E/y4011e06.htm.

Agricultural Market Information System (AMIS), WHEAT: planting and harvesting calendar. Available at: http://www.amis-outlook.org/amis-about/calendars/en/.

Alcamo, J. et al., 2007. A new assessment of climate change impacts on food production shortfalls and water availability in Russia. *Global Environmental Change*, 17(3–4), pp.429–444.

Allen, R.G. et al., 1998. FAO Irrigation and Drainage Paper No. 56. Crop Evapotranspiration (guidelines for computing crop water requirements). *Irrigation and Drainage*, 300(56), p.300. Available at: http://www.kimberly.uidaho.edu/water/fao56/fao56.pdf.

Antokhina, O.Y. et al., 2016. The impact of atmospheric blocking on spatial distributions of summertime precipitation over Eurasia. *IOP Conference Series: Earth and Environmental Science*, 48(1), p.12035.

Bador, M. et al., 2015. Spatial clustering of summer temperature maxima from the CNRM-CM5 climate model ensembles & E-OBS over Europe. *Weather and Climate Extremes*, 9, pp.17–24. Available at: http://dx.doi.org/10.1016/j.wace.2015.05.003.

Barnes, E.A. et al., 2014. Exploring recent trends in Northern Hemisphere blocking.

Geophysical Research Letters, 41(2), pp.638–644.

Barriopedro, D. et al., 2006. A climatology of Northern Hemisphere blocking. *Journal of Climate*, 19(6), pp.1042–1063.

Barriopedro, D. et al., 2011. The Hot Summer of 2010 : Map of Europe. *Science*, Vol. 332(6026), pp.220–224.

Belyaeva, M. & Bokusheva, R., 2018. Will climate change benefit or hurt Russian grain production? A statistical evidence from a panel approach. *Climatic change*, 149(2), pp.205–2017.

Bernard, E. et al., 2013. Clustering of maxima: Spatial dependencies among heavy rainfall in france. *Journal of Climate*, 26(20), pp.7929–7937.

Brouwer, C., Prins, K. & Heibloem, M., 1989. Irrigation Water Management: Irrigation Scheduling. *FAO Land and Water Development Division*, 4(4), p.66. Available at: http://www.fao.org/docrep/t7202e/t7202e07.htm.

Brunner, L., Hegerl, G.C. & Steiner, A.K., 2017. Connecting atmospheric blocking to European temperature extremes in spring. *Journal of Climate*, 30(2), pp.585–594.

Bulgakov, D.S. et al., 2016. Separation of agroclimatic areas for optimal crop growing within the framework of the natural--agricultural zoning of Russia. *Eurasian Soil Science*, 49(9), pp.1049–1060.

Bulygina, O.N. & Razuvaev, V.N., 2012. *Daily Temperature and Precipitation Data for 518 Russian Meteorological Stations.*,

Casanueva, A. et al., 2014. Variability of extreme precipitation over Europe and its relationships with teleconnection patterns. *Hydrology and Earth System Sciences*, 18(2), pp.709–725.

Cheung, H.N. et al., 2013. Revisiting the climatology of atmospheric blocking in the Northern Hemisphere. *Advances in Atmospheric Sciences*, 30(2), pp.397--410.

Coles, S., 2001. *An Introduction to Statistical Modeling of Extreme Values*, Springer. Available at: http://link.springer.com/10.1007/978-1-4471-3675-0.

Cooley, D., Naveau, P. & Poncet, P., 2006. Variograms for spatial max-stable random fields. In *Dependence in Probability and Statistics*. Springer, pp. 373–390. Available at: http://link.springer.com/10.1007/0-387-36062-X_17.

525 Coumou, D., Lehmann, J. & Beckmann, J., 2015. The weakening summer circulation in the
526 Northern Hemisphere mid-latitudes. *Science*, 348(6232), pp.324–327.

527 Daryanto, S., Wang, L. & Jacinthe, P.A., 2016. Global synthesis of drought effects on maize
528 and wheat production. *PLoS ONE*, 11(5), pp.1–15.

529 Dee, D. et al., 2011. The ERA - Interim reanalysis: Configuration and performance of the data
530 assimilation system. *Quaterly Journal of the Royal Meteorological Society*, 137(656),
531 pp.553–597.

532 Dole, R. et al., 2011. Was there a basis for anticipating the 2010 Russian heat wave?
533 *Geophysical Research Letters*, 38(6), pp.1–5.

534 Dronin, N. & Kirilenko, A., 2008. Climate change and food stress in Russia: What if the market
535 transforms as it did during the past century? *Climatic Change*, 86(1–2), pp.123–150.

536 Dunn-Sigouin, E. & Son, S.-W., 2013. Northern hemisphere blocking frequency and duration
537 in the CMIP5 models. *J. Geophys. Res.*, 118(3), pp.1179–1188.

538 Federal Service of Hydrometeorology and Environmental Monitoring, R., 2008. Asessment
539 Report on Climate Change and Its Consequences in Russian Federations. Available at:
540 http://climate2008.igce.ru/v2008/pdf/resume_ob_eng.pdf [Accessed June 28, 2018].

541 Felber, R., Stoeckli, S. & Calanca, P., 2018. Generic calibration of a simple model of diurnal
542 temperature variations for spatial analysis of accumulated degree-days. *International*
543 *Journal of Biometeorology*, 62(4), pp.621–630.

544 Fischer, G., Shah, M. & van Velthuizen, H., 2002. Climate change and agricultural
545 vulnerability. A special report, prepared by IIASA as a contribution to the World Summit
546 on Sustainable Development, Johannesburg. Laxenburg (Austria): IIASA. *IIASA*
547 *Johannesburg*.

548 Folland, C.K. et al., 2009. The summer North Atlantic oscillation: Past, present, and future.
549 *Journal of Climate*, 22(5), pp.1082–1103.

550 Fontana, G. et al., 2015. Early heat waves over Italy and their impacts on durum wheat yields.
551 *Natural Hazards and Earth System Sciences*, 15(7), pp.1631–1637.

552 Food and Agriculture Organization of the United Nations, 2010. FAO cuts wheat production
553 forecast but considers supplies adequate. *August 4*. Available at:
554 http://www.fao.org/news/story/en/item/44570/icode/ [Accessed February 17, 2017].

555 Gentle, J.E., Kaufman, L. & Rousseuw, P.J., 1991. *Finding Groups in Data: An Introduction*
556 *to Cluster Analysis.*, John Wiley & Sons. Available at:
557 http://www.jstor.org/stable/2532178?origin=crossref.

558 Gourdji, S.M., Sibley, A.M. & Lobell, D.B., 2013. Global crop exposure to critical high
559 temperatures in the reproductive period: Historical trends and future projections.
560 *Environmental Research Letters*, 8(2).

561 Grumm, R.H., 2011. The central European and russian heat event of July-August 2010. *Bulletin*
562 *of the American Meteorological Society*, 92(10), pp.1285–1296.

563 Häkkinen, S., Rhines, P.B. & Worthen, D.L., 2011. Atmospheric blocking and Atlantic
564 multidecadal ocean variability. *Science*, 334(6056), pp.655–659. Available at:
565 http://hdl.handle.net/2060/20110008410.

566 Hartigan, J.A., Spath, H. & Ryzin, J. Van, 1981. *Clustering Algorithms*, Wiley New York.
567 Available at: http://www.jstor.org/stable/3151350?origin=crossref.

568 Hartigan, J.A. & Wong, M.A., 1979. Algorithm AS 136: a K-means clustering algorithm. *J*
569 *Royal Stat Soc Series C Appl Stat* , 28, pp.100–108.

570 Irannezhad, M., Chen, D. & KlØve, B., 2016. the Role of Atmospheric Circulation Patterns in
571 Agroclimate Variability in Finland, 1961–2011. *Geografiska Annaler, Series A: Physical*
572 *Geography*, 98(4), pp.287–301.

573 Irannezhad, M. & Kløve, B., 2015. Do atmospheric teleconnection patterns explain variations
574 and trends in thermal growing season parameters in Finland? *International Journal of*
575 *Climatology*, 35(15), pp.4619–4630.

576 Katsafados, P. et al., 2014. Seasonal predictability of the 2010 Russian heat wave. *Natural*
577 *Hazards and Earth System Sciences*, 14(6), pp.1531–1542.

578 Kottek, M. et al., 2006. World map of the Kopen-Geiger climate classification updated.
579 *Meteorologische Zeitschrift*, 15(3), pp.259–263. Available at: http://koeppen-geiger.vu-
580 wien.ac.at/%5CnKottek2006.pdf.

581 Lejenäs, H. & økland, H., 1983. Characteristics of northern hemisphere blocking as determined
582 from a long time series of observational data. *Tellus A*, 35 A(5), pp.350–362.

583 Liefert, W.M. & Liefert, O., 2015. Russia's potential to increase grain production by expanding
584 area. *Eurasian Geography and Economics*, 56(5), pp.505–23.

585 Lupo, A.R. et al., 2014. Studying summer season drought in Western Russia. *Advances in*
586 *Meteorology*, 2014. Available at:
587 http://downloads.hindawi.com/journals/amete/2014/942027.pdf.

588 Matsueda, M., 2011. Predictability of Euro-Russian blocking in summer of 2010. *Geophysical*
589 *Research Letters*, 38(6).

590 Mogensen, V.O., Jensen, H.E. & Rab, A., 1985. Grain Yield , Yield Components , Drought
591 Sensitivity and Water Use Efficiency of Spring Wheat Subjected to Water Stress at
592 Various Growth Stages. *Irrigation Science*, 6, pp.131–140.

593 Mokhov, I.I. & Semenov, V.A., 2016. Weather and Climate Anomalies in Russian Regions
594 Related to Global Climate Change. *Russian Meteorology and Hydrology*, 41(2), pp.84–
595 92. Available at: http://link.springer.com/10.3103/S1068373916020023.

596 Mokhov, I.I. & Timazhev, A. V., 2015. Model assessment of possible changes of atmospheric
597 blockings in the Northern Hemisphere under RCP scenarios of anthropogenic forcings.
598 *Doklady Earth Sciences*, 460(1), pp.63–67. Available at:
599 http://link.springer.com/10.1134/S1028334X15010122.

600 Mokhov, I.I. & Timazhev, A. V, 2017. Assessing the Probability of El Ni no-related Weather
601 and Climate Anomalies in Russian Regions. *Russian Meteorology and Hydrology*, 42(10),
602 pp.635–643.

603 Nicolas, M., Gleadow, R. & Dalling, M., 1984. Effects of Drought and High Temperature on
604 Grain Growth in Wheat. *Australian Journal of Plant Physiology*, 11(6), p.553. Available
605 at: http://www.publish.csiro.au/?paper=PP9840553.

606 Olesen, J.E. et al., 2012. Changes in time of sowing, flowering and maturity of cereals in Europe
607 under climate change. *Food Additives and Contaminants - Part A Chemistry, Analysis,*
608 *Control, Exposure and Risk Assessment*, 29(10), pp.1527–1542.

609 Di Paola, A. et al., 2018. The expansion of wheat thermal suitability of Russia in response to
610 climate change. *Land use policy*, 78, pp.70–77.

611 Park, Y.J. & Ahn, J.B., 2014. Characteristics of atmospheric circulation over east Asia
612 associated with summer blocking. *Journal of Geophysical Research*, 119(2), pp.726–738.

613 Parton, W.J. & Logan, J. a., 1981. A model for diurnal variation in soil and air temperature.
614 *Agricultural Meteorology*, 23, pp.205–216.

615 Peel, M.C., Finlayson, B.L. & McMahon, T.A., 2007. Updated World Map of the Köppen-
616 Geiger Climate Classification. *Hydrol. Earth Systm. Sci. Discuss.*, 4, pp.439–473.

Petoukhov, V. et al., 2013. Quasiresonant amplification of planetary waves and recent Northern Hemisphere weather extremes. *Proceedings of the National Academy of Sciences*, 110(14), pp.5336–5341. Available at: http://www.pnas.org/cgi/doi/10.1073/pnas.1222000110.

Pfahl, S. & Wernli, H., 2012. Quantifying the relevance of atmospheric blocking for co-located temperature extremes in the Northern Hemisphere on (sub-)daily time scales. *Geophysical Research Letters*, 39(12).

Press, W.H. et al., 2007. *Numerical recipes 3rd edition: The art of scientific computing*, Cambridge university press. Available at: http://epubs.siam.org/doi/10.1137/1031025.

Renwick, J.A. & Wallace, J.M., 1996. Relationships between North Pacific Wintertime Blocking, El Niño, and the PNA Pattern. *Monthly Weather Review*, 124(9), pp.2071–2076. Available at: http://journals.ametsoc.org/doi/abs/10.1175/1520-0493%281996%29124%3C2071%3ARBNPWB%3E2.0.CO%3B2.

Ribatet, M., Singleton, R. & Team, R.C., 2011. Spatialextremes: Modelling spatial extremes. *R package version*, pp.1–8.

Rohrer, M. et al., 2018. Representation of extratropical cyclones, blocking anticyclones, and alpine circulation types in multiple reanalyses and model simulations. *Journal of Climate*, 31(8), pp.3009–3031. Available at: http://journals.ametsoc.org/doi/10.1175/JCLI-D-17-0350.1.

Russian Federal State Statistics, S., 2014. *Russia: Statistical Pocket book*, Available at: http://www.gks.ru/free_doc/doc_2014/rus14_eng.pdf [Accessed June 26, 2018].

Russian Federal State Statistics, S., 2016. *Russia in Figures, 2016. Statistical Handbook. Moscow, 543 p.*, Federal State Statistics Service. Available at: http://www.gks.ru/free_doc/doc_2017/rusfig/rus17e.pdf.

Russo, S., Sillmann, J. & Fischer, E.M., 2015. Top ten European heatwaves since 1950 and their occurrence in the coming decades. *Environmental Research Letters*, 10(12), p.124003. Available at: http://dx.doi.org/10.1088/1748-9326/10/12/124003.

Rust, H.W. et al., 2014. Linking teleconnection patterns to European temperature -- A multi-linear regression model. *Meteorol. Z.*, submitted(4), pp.411–423.

Savin, I. et al., 2007. Climatically Optimal Planting Dates (version 1). *JRC Scientific and Technical Reports*, (version 1), p.58.

Schaller, N. et al., 2018. Influence of blocking on Northern European and Western Russian heatwaves in large climate model ensembles. *Environmental Research Letters*, 13(5),

p.54015. Available at: http://stacks.iop.org/1748-9326/13/i=5/a=054015.

Scherrer, S.C. et al., 2006. Two-dimensional indices of atmospheric blocking and their statistical relationship with winter climate patterns in the Euro-Atlantic region. *International Journal of Climatology*, 26(2), pp.233–249.

Schierhorn, F., Faramarzi, M., et al., 2014. Quantifying yield gaps in wheat production in Russia. *Environmental Research Letters*, 9(8), p.084017.

Schierhorn, F., Müller, D., et al., 2014. The potential of Russia to increase its wheat production through cropland expansion and intensification. *Global Food Security*, 3(3–4), pp.133–141. Available at: http://dx.doi.org/10.1016/j.gfs.2014.10.007.

Schneider, A., Musick, J. & Dusek, D., 1969. Efficient wheat irrigation with limited water. *Transactions of the ASAE.*, 12(1), pp.23-0026.

Schneidereit, A. et al., 2012. Large-Scale Flow and the Long-Lasting Blocking High over Russia: Summer 2010. *Monthly Weather Review*, 140(9), pp.2967–2981. Available at: http://journals.ametsoc.org/doi/abs/10.1175/MWR-D-11-00249.1.

Schubert, S.D. et al., 2014. Northern Eurasian heat waves and droughts. *Journal of Climate*, 27(9), pp.3169–3207.

Schwierz, C., Dirren, S. & Davies, H.C., 2004. Forced Waves on a Zonally Aligned Jet Stream. *Journal of the Atmospheric Sciences*, 61(1), pp.73–87.

Shabbar, A., Huang, J. & Higuchi, K., 2001. The relationship between the wintertime North Atlantic oscillation and blocking episodes in the North Atlantic. *International Journal of Climatology*, 21(3), pp.355–369.

Sillmann, J. et al., 2011. Extreme cold winter temperatures in Europe under the influence of North Atlantic atmospheric blocking. *Journal of Climate*, 24(22), pp.5899–58913.

Teixeira, E.I. et al., 2013. Global hot-spots of heat stress on agricultural crops due to climate change. *Agricultural and Forest Meteorology; 2013*, 170, pp.206–215.

Tibaldi, S. et al., 1994. Northern and Southern Hemisphere Seasonal Variability of Blocking Frequency and Predictability. *Monthly Weather Review*, 122(9), pp.1971–2003. Available at: http://journals.ametsoc.org/doi/abs/10.1175/1520-0493%281994%29122%3C1971%3ANASHSV%3E2.0.CO%3B2.

Tibaldi, S. & Molteni, F., 1990. On the operational predictability of blocking. *Tellus A*, 42(3),

679 pp.343–365.

680 Trnka, M. et al., 2014. Adverse weather conditions for European wheat production will become
681 more frequent with climate change. *Nature Climate Change*, 4(7), pp.637–643.

682 Tyrlis, E. & Hoskins, B.J., 2008. Aspects of a Northern Hemisphere Atmospheric Blocking
683 Climatology. *Journal of the Atmospheric Sciences*, 65(5), pp.1638–1652. Available at:
684 http://journals.ametsoc.org/doi/abs/10.1175/2007JAS2337.1.

685 United States Department of Agriculture, F.A.S., 2017. Crop Calendars for Russia Federation.
686 Available at: https://ipad.fas.usda.gov/rssiws/al/crop_calendar/rs.aspx [Accessed June 26,
687 2018].

688 United States Department of Agriculture, F.A.S., 2018. Crop Explorer - Commodity
689 Intelligence Reports - Russian Federation. Available at:
690 https://ipad.fas.usda.gov/cropexplorer/pecad_stories.aspx?regionid=rs&ftype=topstories
691 [Accessed June 29, 2018].

692 United States Department of Agriculture, F.A.S., 2016. Grain, World Markets and Trade.
693 Available at: http://usda.mannlib.cornell.edu/usda/fas/grain-market//2010s/2016/grain-
694 market-12-09-2016.pdf [Accessed June 22, 2018].

695 United States Department of Agriculture, F.A.S., 2006. Russia: Wheat Map. Available at:
696 https://www.usda.gov/oce/weather/pubs/Other/MWCACP/Graphs/russia/russia_wheat.p
697 df [Accessed June 26, 2018].

698 Welton, G., 2011. The Impact of Russia' s 2010 Grain Export Ban. *Oxfam Research Reports*,
699 11(5), p.32.

700 Wheeler, T.R. et al., 2000. Temperature variability and the yield of annual crops. *Agriculture,*
701 *Ecosystems and Environment*, 82(1–3), pp.159–167.

702 Wollenweber, B., Porter, J.R. & Schellberg, J., 2003. Lack of Interaction between Extreme
703 High Temperature Events at Vegetative and Reproductive Growth Stages in wheat.
704 *Journal of Agronomy and Crop Science*, 189(3), pp.142–150.

705 Woollings, T., Harvey, B. & Masato, G., 2014. Arctic warming, atmospheric blocking and cold
706 European winters in CMIP5 models. *Environmental Research Letters*, 9(1), p.014002.
707 Available at: http://stacks.iop.org/1748-
708 9326/9/i=1/a=014002?key=crossref.067e034ecb70a6ed7629f423f58d540e.

709 Wright, C.K., De Beurs, K.M. & Henebry, G.M., 2014. Land surface anomalies preceding the
710 2010 Russian heat wave and a link to the North Atlantic oscillation. *Environmental*

Research Letters, 9(12), p.124015. Available at: http://iopscience.iop.org/1748-9326/9/12/124015/article/.

Zampieri, M. et al., 2017. Wheat yield loss attributable to heat waves , drought and water excess at the global , national and subnational scales. *Environmental Research Letters*, 12(6), p.064008.

Zhang, X., Yang, F. & Santos, J., 2004. RClimDex (1.0) Manual del Usuario. *Climate Research Branch Environment Canada*, 22, p.22. Available at: http://geoportal.ciifen.org/media/filer_public/c4/65/c4658d38-c6ef-4729-9f80-94ff9f9ecb3a/manual_de_inices_climaticos.pdf.

{Bibliography

Figures

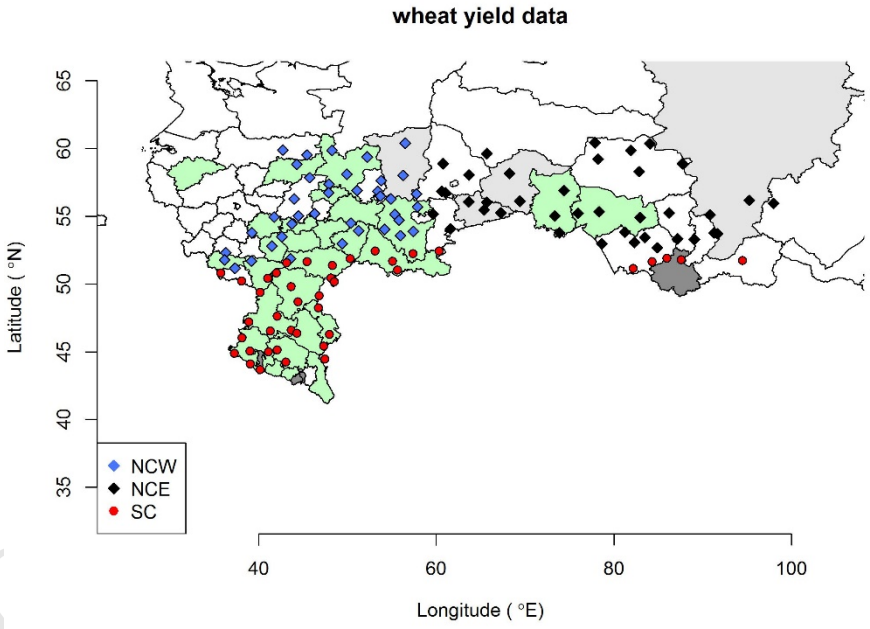

Figure 1: Map of the study area showing the political borders (oblasts, i.e. subjects of the Russian Federation), the location of the weather stations, grouped according to the results of the cluster analysis (blue diamonds: *NCW*; black diamonds: *NCE*; red dots: *SC*). In addition, the maps indicate whether both types of wheat are cultivated (light green), or whether there is a predominance of either winter (dark grey) or spring wheat (light grey).

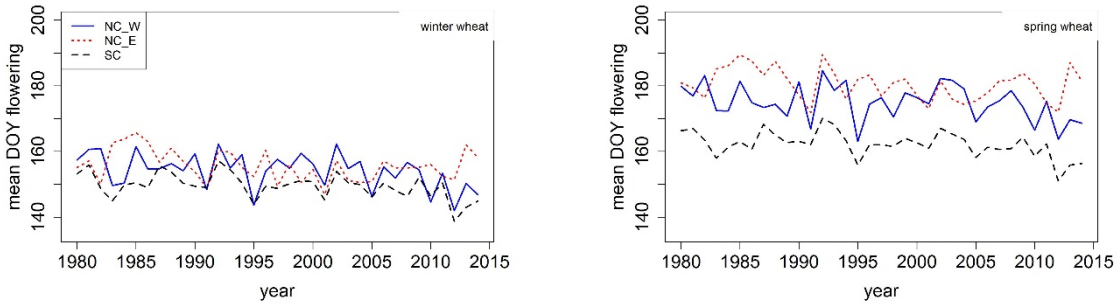

727 **Figure 2: Time series (1980-2014) of the mean date of flowering (day of the year, DOY_{flo}) for *WW* and *SW*,**
728 **spatially averaged for each cluster separately.**
729
730

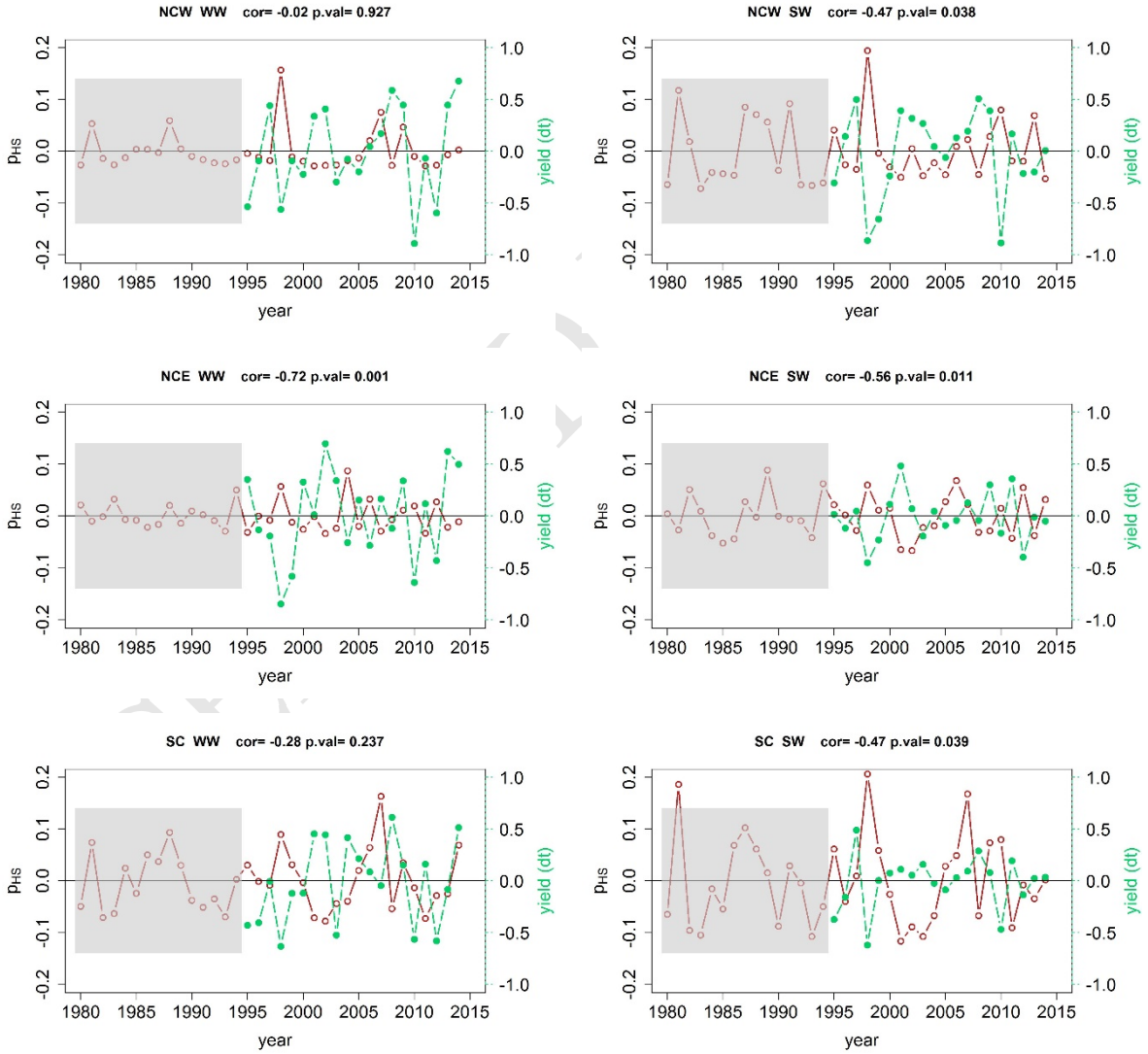

731 **Figure 3: Time series of de-trended mean probability of heat stress (red continuous lines and open dots) and de-trended**
732 **mean wheat yield (green dashed lines and solid dots) in the reproductive period of *WW*, respectively *SW*. Shown from**
733 **top to bottom are the series for the *NCW*, *NCE* and *SC*. Correlation coefficient and statistical significance are indicated**
734 **above each panel. Grey boxes mask the years for which wheat yield data was not available.**

735

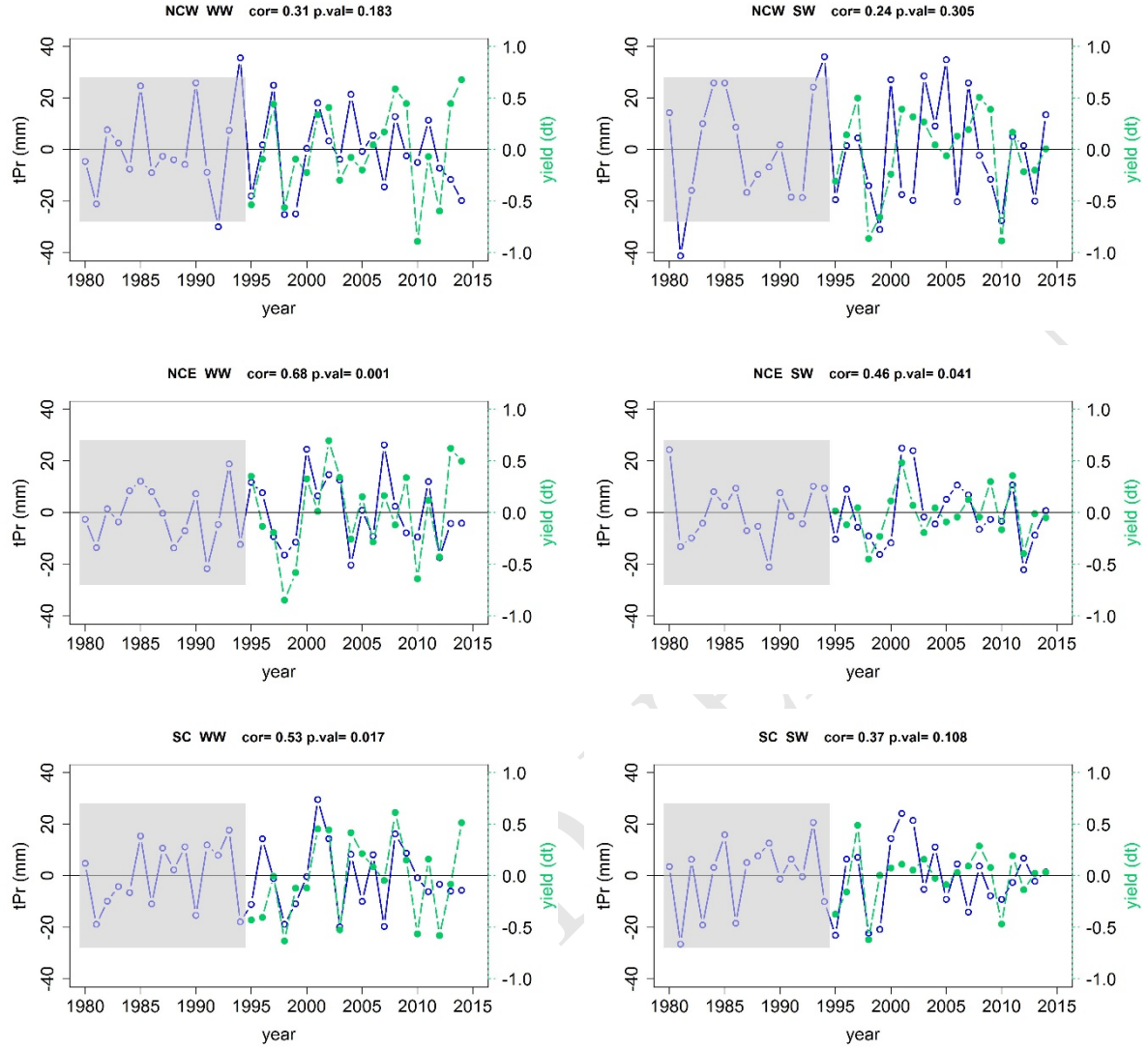

736 **Figure 4: Same as Figure 3 but for de-trended mean precipitation amount (blue lines and open dots) instead of**

737 **probability of heat stress occurrence.**

738

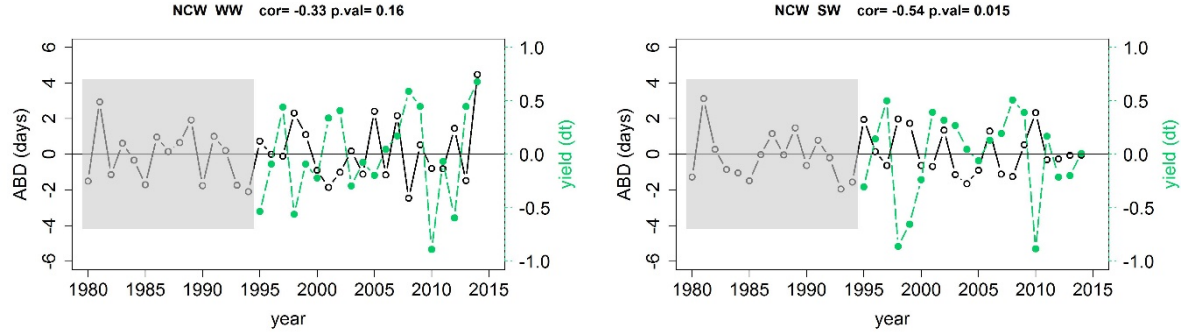

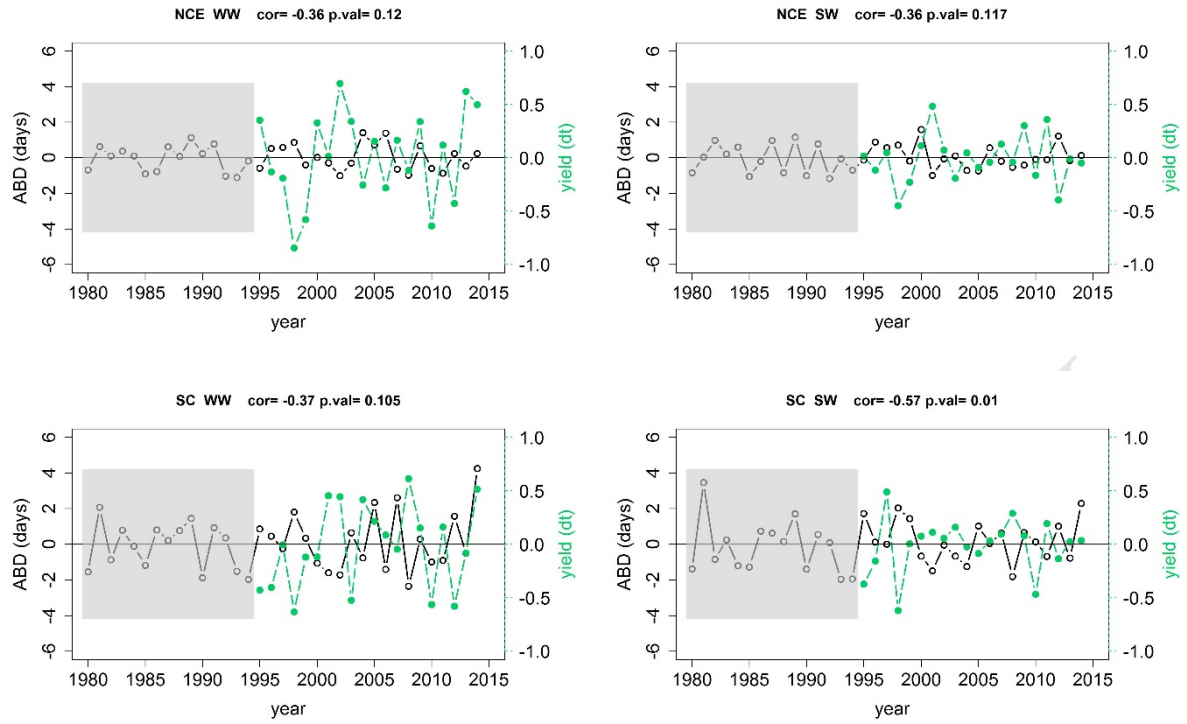

739 **Figure 5: Same as Figure 3 but contrasting the time series of yield (green dashed lines and solid dots) with the time**
740 **series of average number of blocked days (black continuous lines and open dots).**

741 # Appendix

742

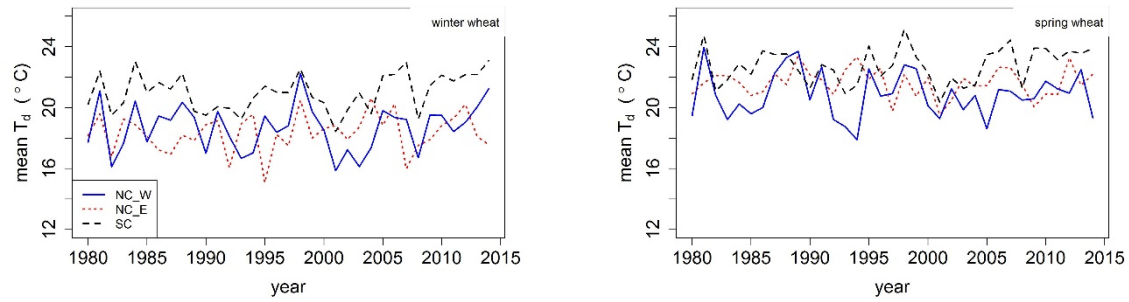

743 **Figure S1: Time series (1980-2014) of the mean daytime temperature (T_{day}) for *WW* and *SW*. The data**
744 **represent mean values over the 31 days around flowering ($DOY_{flo} - 15$ to $DOY_{flo} + 15$), spatially**
745 **averaged for each cluster separately.**

746

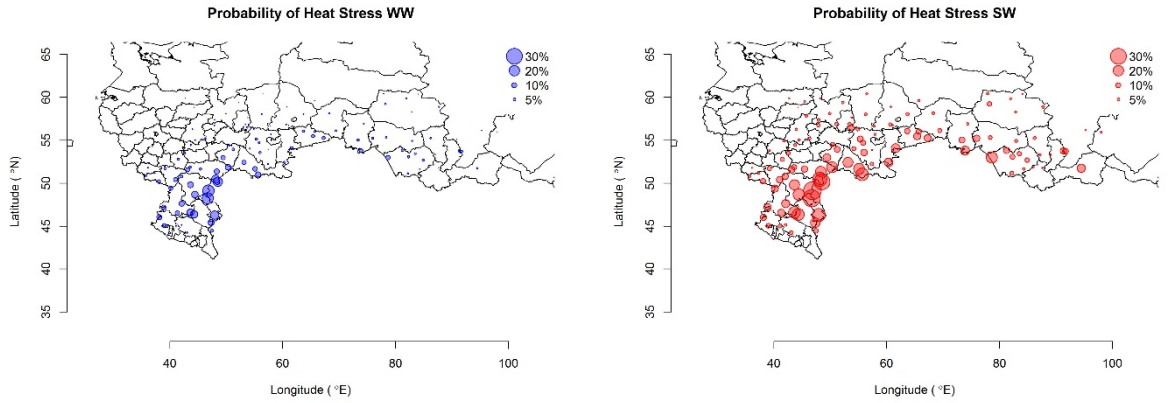

747 **Figure S2: Mean (10980-2014) probability of heat stress occurrence in the 31 days around flowering for *WW***

748 **and *SW*. The size of the dots is is proportional to the probability.**

749

750

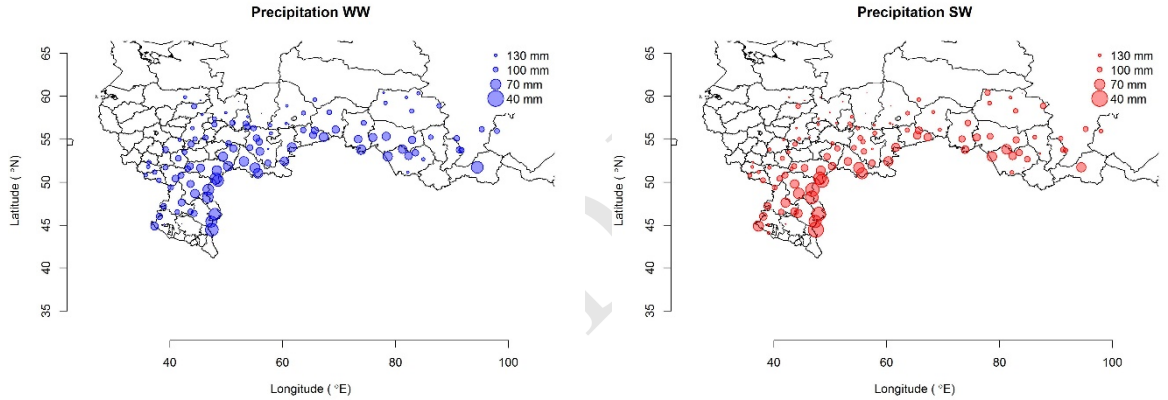

751 **Figure S3: Same as Figure S2 but for the mean total precipitation amount. Note that in this case the size of the dots is**

752 **inversely proportional to precipitation volume.**

753

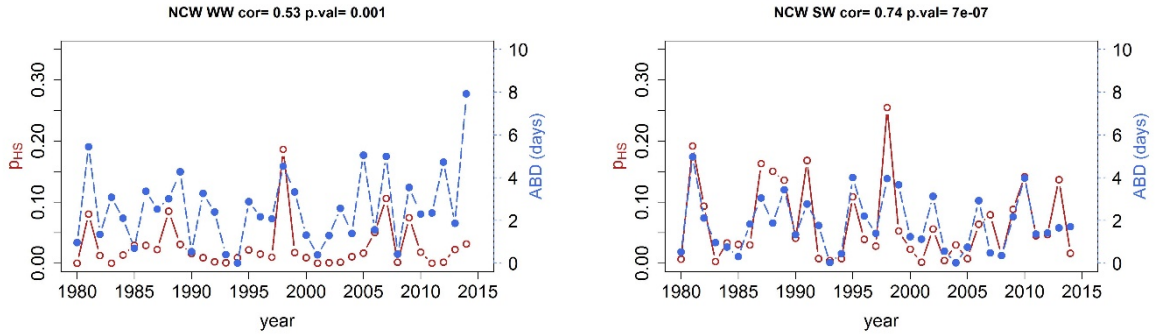

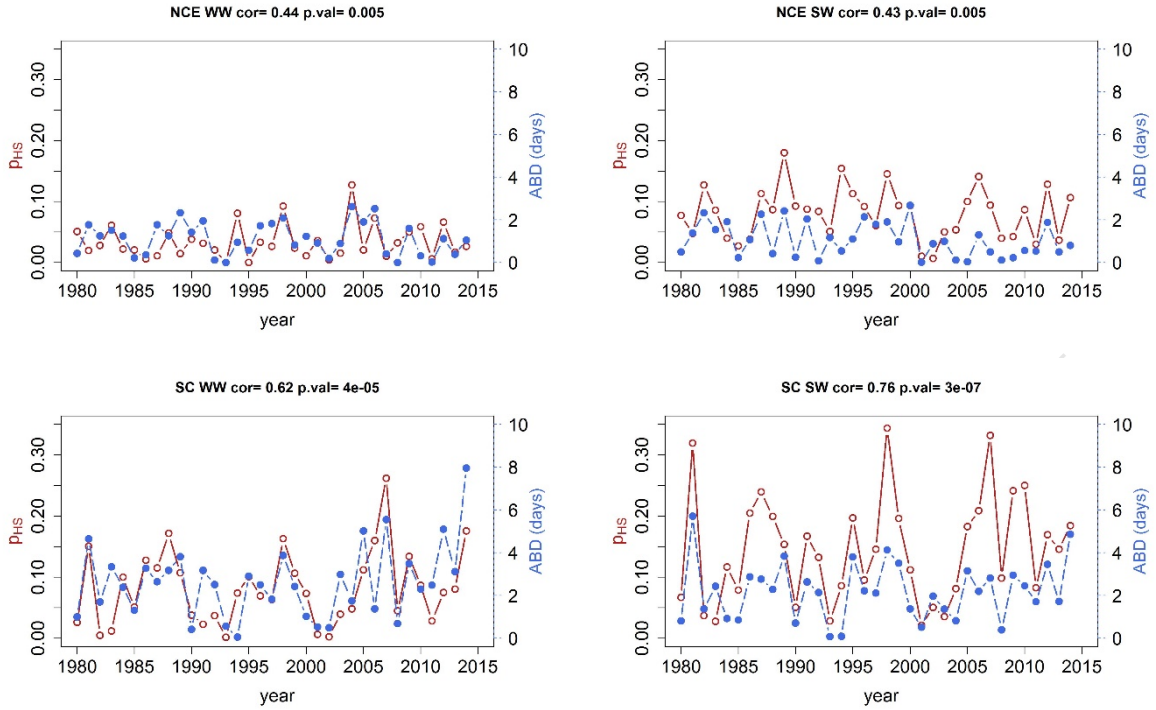

754 **Figure S4: Time series (1980-2014) of the mean *ABD* (blue dashed line and solid dots) and the mean probability of heat**
755 **stress (red continuous line and open dots) 31 days around *WW* and *SW* flowering for *NCW*, *NCE* and *SC*. Correlation**
756 **coefficient and p-value are indicated above each panel.**

757

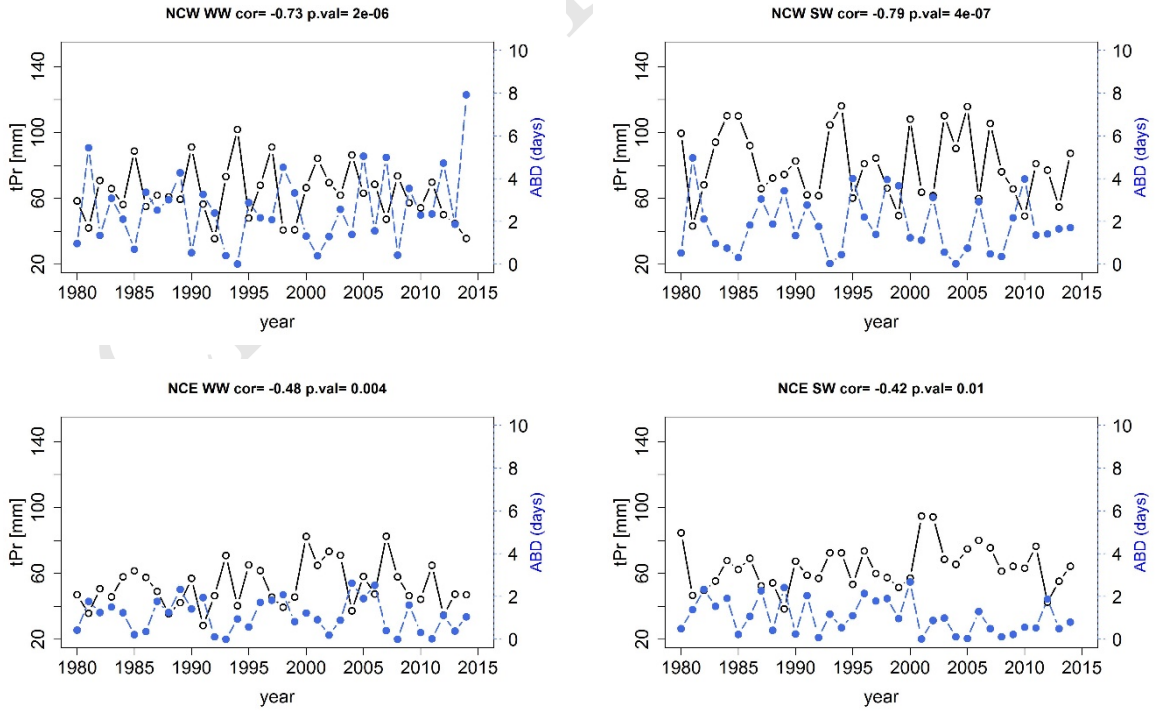

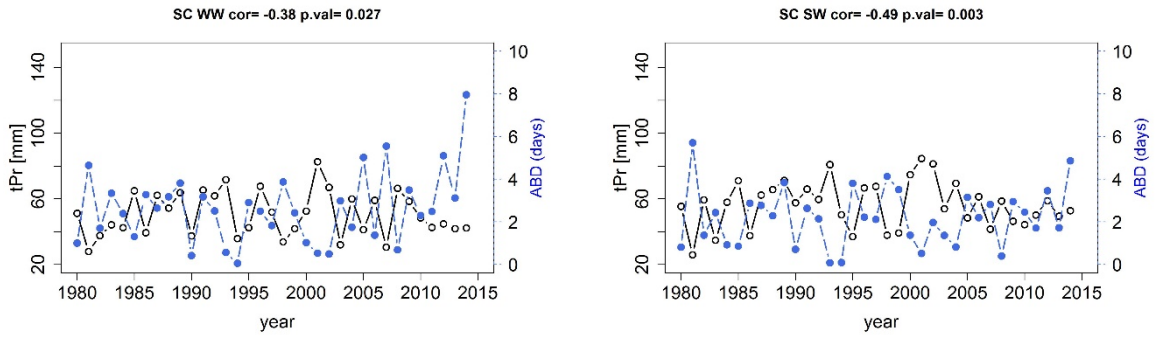

Figure S5: same as Figure S4 but with time series of total precipitation amounts (black continuous lines and open dots) instead of the probability of heat stress occurrence.

Table S1: Spearman rank correlation between probability of heat stress and mean total precipitation amounts in the 31 days around *WW* and *SW* flowering. Bold face: statistically significant results. Significance levels: (*) 10%, (**) 5%, (***) 1%.

Winter wheat				**Spring wheat**		
NCW	*NCE*	*SC*		*NCW*	*NCE*	*SC*
-0.44 (**)	**-0.62 (***)**	**-0.4 (*)**		**-0.63 (***)**	**-0.35 (*)**	**-0.47 (**)**

Table S2: Sensitivity analysis of the correlation between heat stress and yield variations with respect to shifts in the date of flowering. Bold face: statistically significant results. Significance levels: (*) 10%, (**) 5%, (***) 1%.

	Winter wheat				**Spring wheat**		
	NCW	*NCE*	*SC*		*NCW*	*NCE*	*SC*
$DOY_{flo} - 5$	0.02	**-0.65 (**)**	-0.04		**-0.48 (*)**	**-0.48 (*)**	**-0.49 (*)**
reference	-0.02	**-0.72 (**)**	-0.28		**-0.47 (*)**	**-0.56 (*)**	**-0.47 (*)**
$DOY_{flo} + 5$	-0.03	**-0.66 (**)**	**-0.31 (*)**		**-0.46 (*)**	**-0.69 (**)**	**-0.53 (**)**
$DOY_{flo} + 10$	-0.06	**-0.59 (**)**	**-0.37 (*)**		**-0.51 (*)**	**-0.63 (**)**	**-0.55 (**)**

Verification of the Olesen et al. (2012) model of wheat phenology

We assessed the plausibility of the predicted sowing dates for spring wheat by comparing them to data extracted from Savin et al. (2007) and the range of dates given in Agricultural Market

775 Information System (AMIS, 2012), United States Department of Agriculture 2006, 2017,
776 Figure S6).

777 As for the dates of flowering, we compared the estimated dates with the potential heading
778 periods given in United States Department of Agriculture (2006, 2017, Figures S7, S8).
779 According to Acevedo et al. (2002), heading precedes flowering by approximately 10 days.
780 Given that the ranges of possible heading dates indicated in the reports by the United States
781 Department of Agriculture (2006, 2017) extend over more than one month, we simply took
782 these as proxies for the ranges of possible flowering dates.

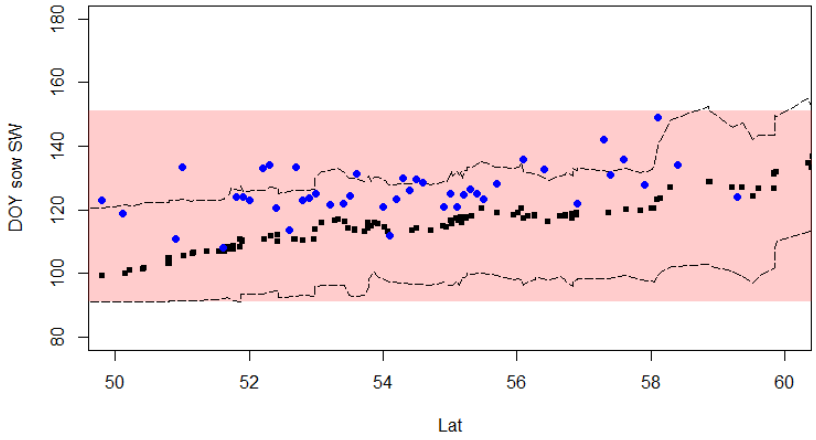

783

784 **Figure S6: Predicted mean sowing dates for spring wheat (black dots) and range (dashed lines) against actual dates**
785 **extracted from Savin et al. (2007) (blue dots). The figure also shows in the background (red stripe) the range of heading**
786 **dates given in United States Department of Agriculture (2006, 2017).**

787

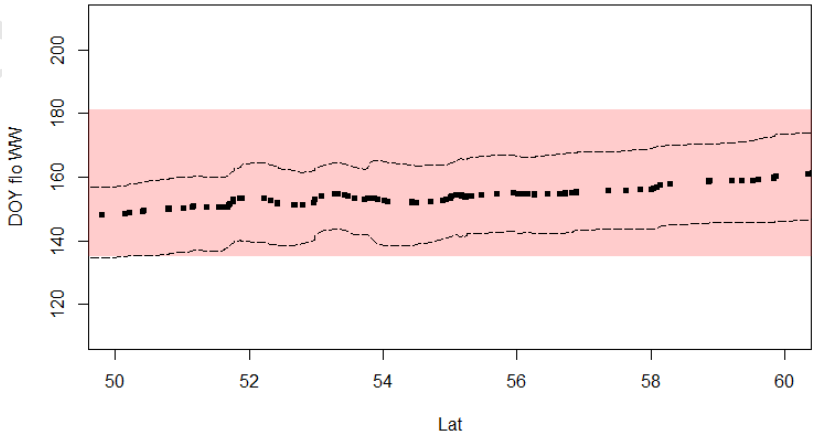

788

Figure S7: Computed range (dashed lines) and mean dates of flowering (dots) for *WW* as a function of latitude. The figure shows in the background (red strip) the range of heading dates given in United States Department of Agriculture (2006, 2017).

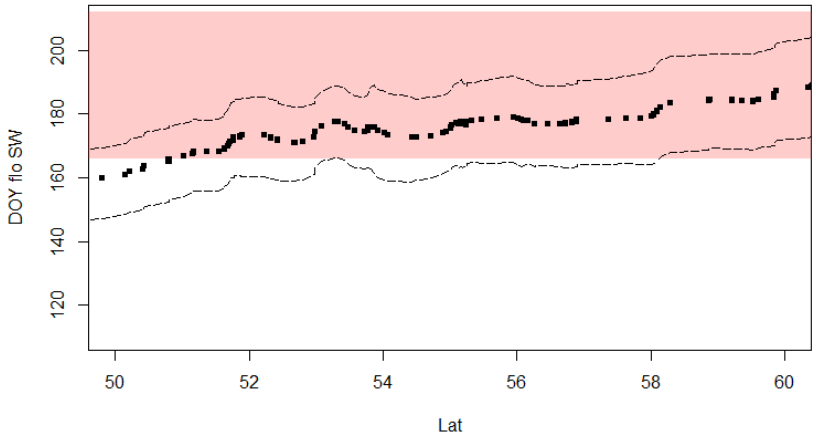

Figure S8: Same as Figure S7, but for *SW*.

As seen in the figures, predictions by the Olesen et al. (2012) model are overall realistic and in line with independent information. The only exception are the flowering dates of *SW* in the very south of the study area. In Southern Russia, winter wheat is the predominant type. It is likely that the overall range of dates available from United States Department of Agriculture (2006, 2017, red stripe Figure S8) is biased toward information available from more northern latitudes.